Smart Energy 6 (2022) 100075

Contents lists available at ScienceDirect

Smart Energy

journal homepage: www.journals.elsevier.com/smart-energy

Assessing the potential of seasonal thermal storage for local energy systems: Case study for a neighborhood in Norway

Hanne Kauko*, Dimitri Pinel, Ingeborg Graabak, Ove Wolfgang

SINTEF Energy Research, Sem Sælands Vei 11, 7034, Trondheim, Norway

ARTICLE INFO

Article history:
Received 30 November 2021
Received in revised form
6 May 2022
Accepted 6 May 2022
Available online xxx

ABSTRACT

District heating has an important role in the shift to carbon-neutral energy systems through enabling the use of heat sources that would otherwise be wasted to cover buildings' heating demands. The availability of many renewable and surplus heat sources is however in opposite phase with the heating demand, creating a demand for seasonal thermal energy storage. This study performs a techno-economic assessment of the heat supply system of a residential area in Norway, where seasonal storage storing excess heat from a waste incineration plant is being planned. A heat supply solution combining seasonal storage and low-temperature district heating was compared with two more conventional alternatives: high-temperature district heating and direct electric heating.

The study shows that the seasonal storage is not cost optimal under the conditions assumed, in particular regarding the electricity market; however, the total costs were only 3% higher compared to electric heating. Seasonal storage additionally allows to reduce the use of peak heating units in the district heating system in the winter, thus reducing the costs and emissions related to heat production, and district heating alone has a significant impact in alleviating the pressure on the power grid. The peak power demand was reduced by 28% when investing to low- or high-temperature district heating, and seasonal storage was shown to enable up to 31% reduction in the peak heating demand. Moreover, it was shown that higher electricity prices in the winter and reduced grid capacity increase the economic viability of the solution and could make it competitive.

1. Introduction

In the light of Europe's ambition to decarbonize its energy system, increasing amounts of variable renewable energy sources will penetrate the energy market. At the same time, due to electrification of transport and industry, the demand for electrical energy will increase tremendously: the share of electricity in final global energy demand is set to double from 19% to 38% within the next 30 years [1]. A narrow-minded focus on electricity as the sole energy carrier will lead to sub-optimal solutions, and correspondingly high investment costs for renewable power production and grid enhancements. Several studies conclude that the additional flexibility that is created by connecting the electricity, heating, cooling, and transport sectors together into a smart energy system can improve the intermittent renewable penetration in the electricity sector and reduce the costs of the transition into a 100% renewable energy system in Europe [2,3].

District heating (DH) can play a particularly important role in alleviating the pressure on the power grid and thus accelerating the transition to a fossil-free energy system [4]. Heating is the largest end-use sector, accounting for approximately half of the total energy consumption in Europe [5]. The majority of heating demand is still covered by fossil fuels, with natural gas boilers being responsible for 66% of space heating and hot water production in Europe [6]. At the same time, there is a huge potential for increased utilization of surplus heat, including both high-temperature industrial surplus heat [7], as well as urban, low-temperature surplus heat sources [8]. District heating is a key enabling technology for enabling the use of such heat sources for covering buildings' heating demands and thus replacing the use of fossil fuels and electricity in urban areas. To enable an efficient utilization of renewable and surplus heat sources however, the present DH systems operating at high temperature levels must undergo a change into low-temperature DH networks, interacting with the surrounding energy system and thus becoming an integrated part of

* Corresponding author.
E-mail address: hanne.kauko@sintef.no (H. Kauko).

https://doi.org/10.1016/j.segy.2022.100075

the future smart energy systems [4].

Thermal energy storage (TES) is another important component in fossil-free energy systems, providing a less costly and more energy friendly alternative for integrating large inflows of fluctuating renewable energy than electric batteries [9]. Heat availability from most renewable and surplus heat sources is nearly in the opposite phase with the heating demand on a yearly basis, and to this end, seasonal thermal energy storage (STES) has a great potential in enabling the storage of heat produced in the summer for use in the winter. Commercially available STES technologies include tank TES, pit TES, borehole TES as well as aquifer TES [10]. For heating systems for neighborhoods or communities, borehole TES is a widely applied solution which is gaining popularity due to its scalability and applicability in a wider range of geological conditions, and ability to store heat at higher temperatures than e.g. aquifer TES.

Borehole STES has so far been mostly applied in neighbourhoods with solar thermal systems [10,11], with Drake Landing Solar Community as the most prominent example [12]. However, the implementation of solar collectors or PV panels increases the investment costs of the heating system significantly [13]. In Sweden, a borehole TES for seasonal storage of industrial waste heat has been implemented [14] but the performance of this system has not met the expectations, partly due to low temperature of the industrial surplus heat.

Another potential heat source for STES is municipal waste incineration. Waste incineration is a common heat source in DH systems in the Nordics, covering 20% of the heat supply for DH systems in Sweden [15] and Denmark [16], 14% in Finland [17], and 48% in Norway [18]. Waste cannot be stored and needs to be burned all year round, leading to a huge amount of high-temperature excess heat available in the summer; while in the winter, costly and often polluting peak heating sources are needed. Consequently, there is a great interest in seasonal storage of this excess heat. Hirvonen and Kosonen [19] have considered the techno-economic feasibility of a borehole TES utilizing excess heat from waste incineration, showing an emission reduction potential of up to 86% in the heat supply for a new residential area in Finland.

Energy system modeling is an important tool for improving the design and performance of urban energy systems with multiple energy sources, and a wide range of tools and approaches exist for this purpose [20]. Different approaches are used for formulation of TES in such models. For instance, Steen et al. [21] and Schutz et al. [22] present multi-layer approaches for modelling TES. In Ref. [21], the focus is on improved description of heat losses, while in Ref. [22], different formulations of TES are compared. Bachmaier et al. [23] have applied a techno-economic optimization tool to study the optimal location, size and operation of TES in a DH system, but have not considered STES. Romanchenko et al. [24] and Buoro et al. [25] study STES in the form of pit and tank TES in their district energy system investment optimization models, however, the resulting STES capacities are relatively small, and the focus is on heat as the only energy carrier. Gabrielli et al. [26] have developed mixed integer linear programming (MILP) methodologies that allow considering a year time horizon with hourly resolution with reduced complexity of the optimization problem for evaluating multi-energy systems with seasonal energy storage, considering lithium batteries, hydrogen storage and hot water tank TES as the storage technologies. Hirvonen and Kosonen [19] on the other hand applied a more detailed physical modeling of a borehole STES connected to a low-temperature DH network using TRNSYS, and carried out a parametric study to find the cost-optimal system configuration.

There are however, to the best of our knowledge, no studies that look at the optimization of both operation and investments of an urban energy system with multiple energy carriers, including seasonal storage of heat, over a planning horizon of several decades. Previous studies including investment in STES either focus on heat as energy carrier or lack the long-term perspective, and the size of the storage results from the optimization and remains limited; hence the potential benefits of a large STES on e.g. limiting grid expansion are not explored. The benefit of analysing cost-efficiency for TES in a multi-energy system model, and not in a partial model for heat supply, is the multi-sectoral trade-offs that exists, e.g. that a more cost-efficient heat-supply system may lead to avoided costs in the electricity grid when the whole energy system is optimized jointly.

This study considers Furuset, a suburban residential area in Oslo, where a micro energy system minimizing energy imports from the surrounding energy system is being planned. A central part of the plan is a borehole TES storing surplus heat from the city's waste incineration plant in the summer, supplying heat to the buildings at Furuset through a local low-temperature DH network during the heating season. Furuset is located in an area with exceptionally good capacity in the power grid; however, showcasing the advantages with low-temperature DH and STES is highly important considering other new neighbourhoods and development areas in Norway and globally. In Norway, direct electric heating is the dominating solution for supplying buildings' heating demands, and the share of DH is currently only 4% of the total heat supply [27]. With the high ambitions for electrification of for instance transport, the importance of DH in reducing the burden on the power grid is increasing. With waste incineration being such common heat source for DH in Norway, the potential for utilizing the excess heat in the summer is enormous. Considering the high initial investment costs for STES, studies demonstrating the benefits are urgently needed.

The main objective of the present study is thus to quantify the energetic and economic benefits of the low-temperature DH system with STES, and to show the potential of such a system in reducing peak loads in the surrounding energy system. The low-temperature DH system with STES is compared with conventional high-temperature DH and direct electric heating using an in-house modeling tool for local multi-energy systems, allowing both investment and operational optimization. For the purposes of the present study, the modeling framework was extended with a module for STES. The main research questions addressed in the study are:

1. What is the potential of low-temperature DH and STES in reducing peak demands for DH and electricity;
2. What is the economic feasibility of multi-energy systems with STES compared with high-temperature DH and direct electric heating; and
3. What is the relevance of STES in Norway and the rest of Europe in the context of the decarbonization goals and future smart energy systems.

2. Methodology

The tool used for modeling the energy system at Furuset is called Integrate,[1] which is a software for the optimal planning and operation of energy systems considering multiple energy carriers (electricity, heat, cooling, biomass, waste, natural gas, oil and hydrogen). It can be used with various temporal and spatial resolutions to model energy systems from continental to local level. The model finds the selection of investment options that minimize total

[1] https://www.sintef.no/en/software/integrate/.

system cost and their timing in a given time horizon. A detailed description of the tool, previously known as eTransport, can be found in Ref. [28] and this section presents only the main elements, relevant for the present study.

Fig. 1 presents the structure of the program. First, several optimizations of the operation of the energy system are performed at hourly resolution for the existing energy system and all the allowed combinations of alternative investments and periods within the studied time horizon using a MILP approach. Subsequently, dynamic programming (DP) is applied to find the optimal investment plan (optimal solution and a few near-optimal). This approach varies from the more traditional approaches, where LP or MILP optimization models can invest linearly in the technologies, but has some advantages. Indeed, it enables to model non-linear, non-convex effects in the investment optimization (implementation of learning effects for instance). Moreover, investment in defined capacities is a better representation of the problematic of investment in technologies in building projects (which come with defined capacities).

The program has a graphical user interface in Microsoft Visio, and uses AMPL for solving the operational optimization and C++ for the investment DP. The representation of the energy system model for Furuset in Visio is shown in Fig. 2. Each component (load, energy source, DH pipe etc.) in the model is added via drag-and-drop functionality. Parameters regarding demand and output, as well as the investment option and planning period the component is a part of, are specified through a pop-up menu. Integrate has a modular structure, which allows to expand the technologies that are modeled based on the demand, such as with the STES module applied in the present study. Instances of various technology modules are used to represent a given energy system as well as the possible future investments.

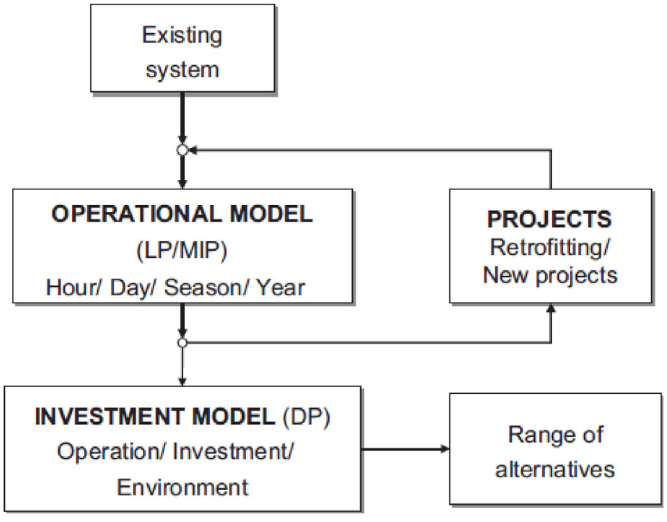

Fig. 1. Structure of the Integrate model. Reproduced from [28].

2.1. Description of the operational optimization

The operational model presented in this section corresponds to the case investigated in the present study. The operational optimization is performed for a selected number of representative days in a year with hourly resolution. The optimization is carried out in the first stage for all the possible combinations of technologies and for all investment periods. Many of the modules available in Integrate were not used in this study, and their contributions to the objective function and constraints are thus not presented here. With the modules used in our case study, the objective function is:

$$min\ c^{ope}_{S_\pi,\pi} = \sum_{\xi}\sigma_\xi\left(\sum_{t_\xi}\left(P^{el}_{t_\xi}\cdot y^{el,imp}_{t_\xi} + \sum_{b}\left(P^{el,def}_{t_\xi,b}\cdot y^{el,def}_{t_\xi,b} + P^{DH,imp}_{t_\xi}\cdot q^{DH,imp}_{t_\xi,b} + P^{SH,def}_{t_\xi}\cdot q^{SH,def}_{t_\xi,b} + P^{DHW,def}_{t_\xi}\cdot q^{DHW,def}_{t_\xi,b}\right) + C^{DH}_{\xi}\right)\right) \quad (1)$$

where S_π are identifiers for the possible combinations of investment options (system states) in period π and $c^{ope}_{S_\pi,\pi}$ is the operational cost of the given state in the given period. Each period has several segments ξ, corresponding in our case to seasons, and several time steps t_ξ within each segment. $P^{el}_{t_\xi}$ and $y^{el,imp}_{t_\xi}$ are respectively the cost and amount of electricity imports; $P^{el,def}_{t_\xi}$, $y^{el,def}_{t_\xi,b}$ the penalty cost and amount of deficit of electricity in building b. Similarly, $P^{DH,imp}_{t_\xi}$ and $q^{DH,imp}_{t_\xi,b}$ are the cost and amount of DH imports, and $P^{SH,def}_{t_\xi}$, $q^{SH,def}_{t_\xi}$, $P^{DHW,def}_{t_\xi}$ and $q^{DHW,def}_{t_\xi,b}$ are the penalty cost and amount of deficit for space heating (SH) and domestic hot water (DHW). C^{DH}_{ξ} are the penalty costs associated with the district heating grid, presented in section 2.3.1.

Each building is represented by its electrical, SH and DHW load and its load balance: $\forall b \in \mathcal{B}, \forall t_\xi$

$$y^{el,imp}_{t_\xi,b} + y^{el,def}_{t_\xi,b} = L^{el}_{t_\xi,b} \quad (2)$$

$$y^{SH,imp}_{t_\xi,b} + y^{SH,def}_{t_\xi,b} = L^{SH}_{t_\xi,b} \quad (3)$$

$$y^{DHW,imp}_{t_\xi,b} + y^{DHW,def}_{t_\xi,b} = L^{DHW}_{t_\xi,b} \quad (4)$$

In addition to the energy balances of the loads, each component of the network within the modeled area has an energy balance as well. Those balances represent the flow of energy within and in between the networks (and their components).

The import of electricity and DH are limited: $\forall t_\xi$

$$y^{el,imp}_{t_\xi} \le Y^{max}_{t_\xi} \quad (5)$$

$$q^{heat,imp}_{t_\xi} \le Q^{max}_{t_\xi} \quad (6)$$

where $Y^{max}_{t_\xi}$ is the maximum electricity import from the grid and $Q^{max}_{t_\xi}$ the maximum heat import. In our case, the investment in a larger transformer is an investment option, so the maximum electricity import will be different in the operational optimizations for the different system states needed in the investment layer.

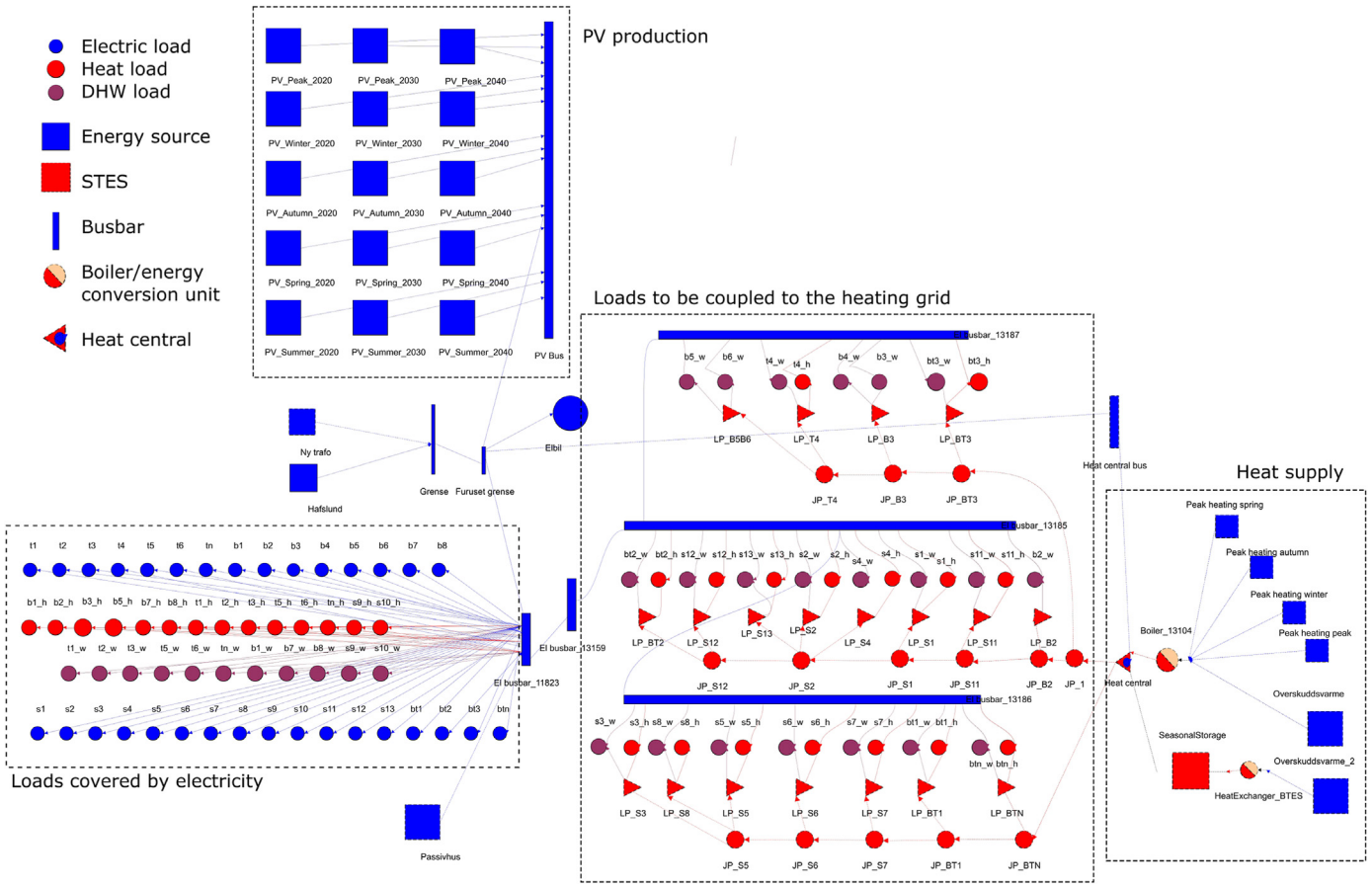

Fig. 2. Integrate-model of the energy system at Furuset.

2.2. Description of the investment optimization

The investment part finds the optimal investment plan based on the available options' investment costs and the operating costs of all the combinations of technologies resulting from the operational optimization. The number of possible combinations increases exponentially with each additional investment option. In order to limit this number, different investment logics can be defined:

- **Mutually exclusive alternatives:** the default investment logic; two investment alternatives are mutually exclusive, i.e. only one of them can be chosen at a time.
- **Time window for investments:** defines the periods in which a given alternative can be chosen.
- **Dependent alternatives:** some alternatives require another alternative to be invested in during the same or a previous period.
- **Necessary alternatives:** a set of investment alternatives where at least one of the alternatives must be carried out within a specified year. Several sets for necessary alternatives can be defined for each year.

The objective of the DP minimizes the discounted present value of all costs, minus the scrap value of new investments. For all investment periods π except the last one we have:

$$C^*_\pi(S_\pi) = min\left\{\delta^{\pi-\Pi_{start}}\left(\sum_{\tau\in\{1,\ldots,\Pi_{step}\}}\delta^{\tau-1}c^{ope}_{S_\pi,\pi}+\sum_{d\in D}c^{inv}_d I_{d\pi}\right)+C^*_{\pi+1}(S_{\pi+1})\right\} \tag{7}$$

where the investment periods are defined by a starting year Π_{start}, end year Π_{end} and a number of years in each period Π_{step}. C^*_π is the minimum net present value in period π. δ is the annual discount factor defined as $\frac{1}{1+r}$, where r is the rate of return. c^{inv}_d is the investment cost of investment option d, $I_{d\pi}$ is a binary parameter which identifies if the investment is performed in the given period and system state.

In the last investment period, we need to account for the residual values of the investments φ:

$$C^*_\pi(S_\pi) = min\left\{ \delta^{\pi-\Pi_{start}} \left(\sum_{\tau\in\{1,\dots,\Pi_{step}\}} \delta^{\tau-1} c^{ope}_{S_\pi,\pi} + \sum_{d\in D} c^{inv}_d I_{d\pi} \right) - \delta^{\Pi_{end}+\Pi_{step}-\Pi_{start}} \varphi + C^*_{\pi+1}(S_{\pi+1}) \right\} \tag{8}$$

In addition, for the possible combinations of investment options (system states) we have:

$$S_{\pi+1} = S_\pi + \sum_{d\in D} 2^{ord(d)-1}(I_{d\pi} - I^{scrap}_{d\pi}) \tag{9}$$

$$\varphi = \sum_{\pi\in[\Pi_{start},\Pi_{end}]} \sum_{d\in D} c^{inv}_d I_{d\pi} max\left\{0; 1 - \frac{\Pi_{end} - \pi + \Pi_{step}}{\lambda_d}\right\} \tag{10}$$

where λ_d is the lifetime of investment option d.

$$C^*_{\Pi_{end}+1} = 0 \tag{11}$$

$$S_{\Pi_{Start}} = 0 \tag{12}$$

The DP algorithm progresses backwards through all periods and possible system states within a period to find the optimal investment plan. Once at the starting period, the optimal investment plan is the path with the lowest net present value. Additional "sub-optimal" investment plans can be found, as many as defined by the user, by running the DP algorithm again with an additional constraint stating that the state in the last period of the investment plan with directly higher rank is infeasible.

2.3. Relevant modules

2.3.1. District heating module

The DH module in Integrate is described in more detail in Refs. [29,30], and here only the main features are given. The DH module includes production points for heat input, junction points, and load points, as well as pipelines connecting the network points. A pipeline contains both the supply and return flow, and reversal of the flow direction is also allowed. The total heat load in the network consists of the SH and DHW loads attached to load points, and heat losses.

The objective of the DH module is to satisfy the demand with minimum heat deficit. In addition to heat deficit at production points and loads, dumping of heat at the production points is penalized. The contribution to the overall objective function is then:

$$C^{DH}_\xi = \sum_{p,t_\xi} q^{DH,dump}_{p,t_\xi} \cdot P^{DH,dump}_{p,t_\xi} + \sum_{p,t_\xi} q^{DH,def}_{p,t_\xi} \cdot P^{DH,def}_{p,t_\xi} + \sum_{b,t_\xi} q^{DH,def}_{b,t_\xi} \cdot P^{DH,def}_{b,t_\xi} \tag{13}$$

where $q^{DH,dump}_{p,t_\xi}$ is dumped heat, $q^{DH,def}_{p,t_\xi}/q^{DH,def}_{b,t_\xi}$ is heat deficit at production/load points; and $P^{DH,dump}_{p,t_\xi}, P^{DH,def}_{p,t_\xi}$ and $P^{DH,def}_{b,t_\xi}$ are the corresponding penalty costs.

At the production points p, the module imports heat from the surrounding energy system and available heat sources, depending on the demand. The demand is defined by the variable q_{less} containing both the heat demand of all the load points connected to the network, as well as the heat losses. The required heat import at each production point p is summed over all the pipes connected to the point:

$$q^{heat,imp}_{t_\xi,p} = \sum_{(p,i)\in DH_{pipes}} q_{less,[p,i,"back","this",t_\xi]} \tag{14}$$

where "back" denotes the return line and "this" the end of the pipe closest to the production point.

The heat losses are calculated for supply flow only, and added to the q_{less} variable at the end of each pipe connecting two network points (i, j):

$$q_{less[i,j,"out","far",t_\xi]} = q_{less[i,j,"out","this",t_\xi]} + l_{pipe[i,j]} \cdot (T_{supply} - T_{ground}) \cdot k_{loss[i,j]}; \tag{15}$$

where "out" denotes the supply line and "this"/"far" denote the pipe ends closest/farthest away from the production point, respectively. $l_{pipe[i,j]}$ is the pipe length, T_{supply} is the supply temperature and T_{ground} the ground temperature, and $k_{loss[i,j]}$ is a heat loss factor.

The heat load (SH or DHW) is added to the q_{less} variable at the far end of each pipe connected to a load point (building) b:

$$\sum_{(i,b)\in DH_{pipes}} q_{less[i,b,"back","far",t_\xi]} = \sum_{(i,b)\in DH_{pipes}} q_{less[i,b,"out","far",t_\xi]} + \sum_{(l,p)\in Net2load} L_{t_\xi,b} \tag{16}$$

where "back" denotes the return line, and DH_{pipes} is the set of pipelines in the network. The returning flow in the pipes thus contains the accumulated heat losses from the supply pipes, as well as the requested heat load at the load points.

To preserve linearity, the supply and return temperatures are set as parameters, while the volume flow of water is a variable. The supply and return temperatures are however allowed to have different values in different seasons to enable a more realistic calculation of heat losses and pumping power. The following constraint makes sure that the water flow is sufficient to cover the demand of load b, at the given supply and return temperatures:

$$q_{less[i,b,"out","far",t_\xi]} + L_{t_\xi,b} + y^{def}_{t_\xi,b} \le C_p \cdot (T_{supply} - T_{return}) \cdot v_{i,b,t_\xi}, \tag{17}$$

where v is the volume flow of water in the pipe (i, b), C_p is the specific heat capacity, and T_{return} is the return temperature.

The required pumping power depends on the pressure drop at the customer substations and in pipes. Pumping power due to pressure drop in pipes has a cubic dependency on the volume flow, and to be able to represent this in Integrate, a piece-wise linear approximation using non-dimensional variables was applied, explained in detail in Ref. [29]. The pumping power is represented as an electrical load in the system, located at the production points, representing the heat central(s) in the system.

The module does not consider the temperature levels for heat exchange at the customer substations or at the heat supply points, but only the amount of energy requested by and supplied into the network. This applies also to TES units attached to the network.

2.3.2. Seasonal thermal energy storage module

Including the operation of seasonal energy storage in optimization models in order to study its techno-economic feasibility can be complex. Energy systems, especially systems including renewable energy sources, require at least an hourly resolution while the

energy planning problem calls for a long time horizon, resulting in unreasonably long computation times. Different approaches, such as clustering have been presented to deal with this issue [26].

In Integrate, the STES is modeled by assuming a certain required amount of heat to be charged, and certain allowed amount of heat to be discharged in the different seasons, taking into account heat losses. The allowed amount of heat to be charged/discharged per representative day is thus obtained by dividing the amount of heat available per season by the number of days belonging to the season.

The daily allowed amount of heat flow to/from a storage unit s is determined by parameter Q_s,*daily*, which is negative for discharging and positive for charging, and given as a share of the total storage capacity Q_s,*tot*. The total amount of heat charged and discharged over a 24-h period is then defined by

$$\begin{aligned} \sum_{t_\xi}\left(q_{charge,s,t_\xi} + y^{def}_{t_\xi,s} - y^{dump}_{t_\xi,s}\right) &= \max\left(0, Q_{daily,s} \cdot Q_{s,tot}\right) \\ \sum_{t_\xi}\left(q_{discharge,s,t_\xi} + y^{dump}_{t_\xi,s}\right) &\le \max\left(0, -Q_{daily,s} \cdot Q_{s,tot}\right) \end{aligned} \tag{18}$$

where $y^{def}_{t_\xi,s}$ represents deficit of heat, and $y^{heat,dump}_{t_\xi,s}$ dumping of heat. q_{charge,s,t_ξ} and $q_{discharge,s,t_\xi}$ are the charging and discharging rates, respectively, with certain allowed maximum values. The storage is charged via a connection to a heat source, and discharged to a heat network or directly to a load. A more detailed description of the STES module in Integrate can be found in Ref. [31].

3. Case study description

Furuset is a multi-functional local neighborhood center in the eastern part of Oslo which incorporates about 3.800 residential units built in the 1970s. It is a pilot area within the research center for Zero Emission Neighborhoods in smart cities (FME ZEN) [32]. Within the coming years, the area will be extended with 1700–2300 apartments and new commercial buildings, and upgraded with new energy infrastructure as well as arrangements for green mobility. To minimize the total and peak energy demands from the surrounding energy system, a large-scale demonstration project combining various solutions for local production of heat and electricity has been launched. Fig. 3 illustrates the concept.

The heating demand of the existing buildings is currently covered by direct electric heating. To supply heat for the new buildings, the plan is to establish a low-temperature DH network in combination with a high-temperature borehole STES. The storage will be charged with excess heat from a nearby waste incineration plant in the summer, and discharged to the local low-temperature heating network in the winter. The remaining heat demand will be covered from the main DH network.

Table 1
The development in annual heat and electricity demands at Furuset from 2020 to 2049.

	Energy demand [GWh/year]		
	2020	2030	2049
Electricity specific	23.5	26.1	32.4
Charging of electric vehicles	0.75	3.1	5.7
Heating (SH and DHW)	24.1	28.5	31.9

To evaluate the benefits of low-temperature DH and STES in reducing peak energy demands from the surrounding energy system, this solution is compared with two other heat supply alternatives: direct electric heating for entire Furuset, and conventional high-temperature DH. Note that heating solutions based on DH applies only to the share of the building mass that will be connected to the planned heating network (see Fig. 2), corresponding to 47% of the total heating demand.

3.1. Energy demand

For the investment analysis, a time horizon from 2020 until 2049 was considered, divided in three periods: 2020–2029, 2030–2039 and 2040–2049. Within this horizon the energy demand at Furuset will grow owing to the increase in building mass and the expected share of electric vehicles, as is shown in Table 1. In the model, the increase in demand was accounted with scaling factors for the different energy demands (SH, DHW, electricity) for each period. The development in demand for heating and electricity for the different buildings at Furuset, as well as the calculation of the scaling factors, is presented in detail in Ref. [34].

For the operational optimization, five representative days inside a year were considered: spring, summer, autumn, winter and peak. Table 2 shows the days belonging to each season. To obtain hourly demand profiles for the representative days for the different buildings at Furuset, yearly demand profiles were first generated using a load profile generator tool [35]. The annual profile was then

Table 2
The selected seasons (representative days), and the days belonging to each season.

	From date	To date	Except	Number of days
Spring	24 Mar	14 May		52
Summer	15 May	18 Sep		127
Autumn	19 Sep	19 Nov		62
Winter	20 Nov	23 Mar	23 Jan	123
Peak	23 Jan	23 Jan		1

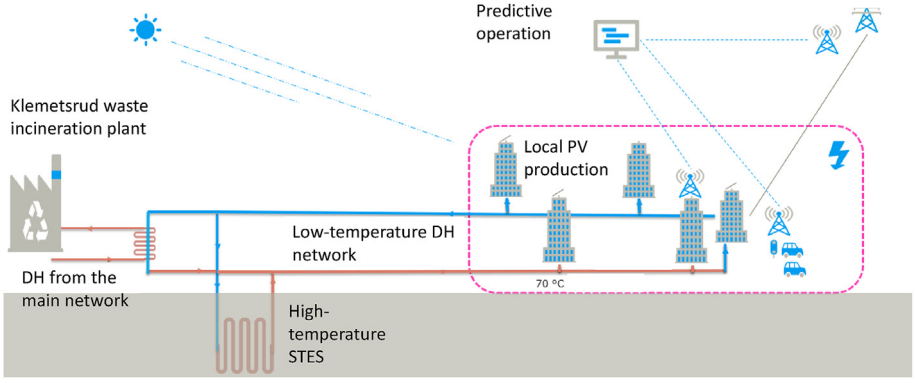

Fig. 3. Illustration of the micro energy system concept at Furuset [33].

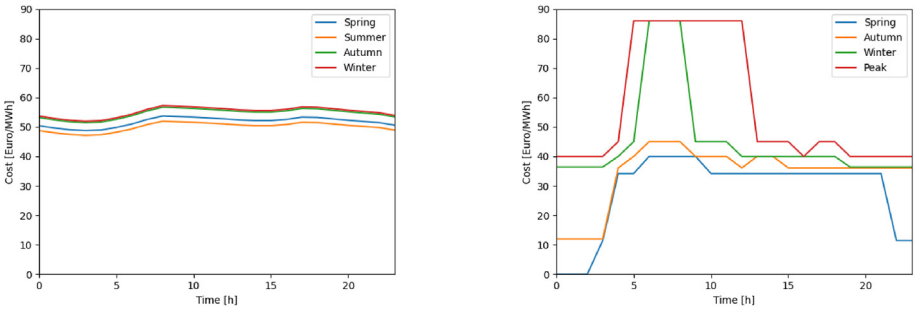

Fig. 4. Costs for (a) electricity and (b) DH for the different representative days.

applied to generate an average daily profile for each building, season and type of energy demand; as well as to calculate scaling factors for the different seasons. Integrate applies identical demand profiles for each representative day, multiplied by a scaling factor to obtain the correct average demand for each season. The daily energy demand profiles for the different energy carriers can be found in Ref. [34].

3.2. Energy costs

3.2.1. Electricity

The end-user price for electricity consists of the power price, grid tariff, as well as taxes and charges. Some of the taxes and charges are not considered as socio-economic costs, and are thus not included in the cost of using electricity.

The Norwegian Directorate for Water Resources and Energy (NVE) has established different scenarios for the future power prices in Norway [36]. Some of the scenarios point towards increased and some towards decreased power prices, and in lack of better knowledge, historic data from Nord Pool for Oslo from 2004 to 2018 was used as a starting point. The average price for each of the 24 h of the day across these 15 years, and our defined seasons, was calculated.

Similarly, for the future grid tariffs, some scenarios point towards increased tariffs due to the required expansion of the power grid with the increasing demand [37]; while some scenarios point towards reduced tariffs as the costs will be divided among a larger number of users [38]. In this study, we used statistical prices for grid tariffs for households, obtained from the grid operator. Electric boilers and heat pumps in the DH network represent dispatchable loads, and for these units, reduced grid tariffs were applied. Fig. 4 (a) shows the power prices over 24 h for the different seasons. For the peak day, the same prices were assumed as in the winter.

3.2.2. District heating

The socio-economic costs of heat delivery to Furuset is the extra cost that incurs for the DH system of Oslo as a result of the deliveries. The cost for DH has thus been set by estimating which technologies will be used in the DH system if more heat is to be produced in a given hour and season. This corresponds to the heating unit with the highest operational cost in operation at a given time. The main heat generation units include waste incineration, electric boilers, heat pumps, as well as boilers using pellets, biodiesel and gas. The share of heat generation from each unit varies throughout the year, and details are given in Table 13 in the appendix.

In the summer, there is excess heat from the waste incineration plant, and the heat costs for this season are therefore set to zero. Fig. 4 (b) shows the costs for the remaining seasons, calculated from the basis of data from the DH supplier on the use of different technologies over the year and price statistics for the different energy sources.

3.3. Local infrastructure

3.3.1. Heating network

Heat supply through DH at Furuset requires both a local piping network and customer substations, as well as a connection to the city's main DH network, approximately 3 km away. The total length of the local heating network is 2400 m. A load point in the modeled network corresponds either to a group of buildings (e.g. a housing cooperative), or a larger single building (e.g. a school).

For the low-temperature DH case, constant supply/return temperatures of 70/50 °C were applied throughout the year. For the high-temperature DH case, weather compensated supply temperature was applied, with a value ranging from 90 to 110 °C, depending on the season. The return temperature was set to 60/50 °C during summer/rest of the year. The heat loss factor was set at 0.75 W/(mK), yielding heat losses of 5.6% at a supply temperature of 70 °C and a ground temperature of 5 °C.

3.3.2. Seasonal thermal energy storage

The planned size of the borehole TES is approximately 390 boreholes with a depth of 200 m each, yielding a total storage capacity of 13 GWh based on information from the DH supplier. The assumed annual heat losses are 5 GWh, which yields 8 GWh of heat available for heating the neighborhood. The storage was assumed to be charged entirely during the summer, and discharged during the remaining seasons. Table 3 shows the allowed charging and discharging of the STES per season in the base case. Allocation of heat available for discharging during the heating seasons was based on the assumption that most of the heat would be used during autumn and winter, while in the spring, the temperature of the storage is lower and thus a smaller share of the heat demand can be covered by the storage. The maximum heat flow rate for charging/discharging was set to 4.27/4 MW based on input from the DH supplier.

3.3.3. Local power production

For local power production, two scenarios were considered: with and without building-integrated PV production, referred to as PV and ~~PV~~, respectively, in order to analyse its potential interplay for the techno-economical viability of the STES solution compared to a grid reinforcement. With PV included, we consider a gradual PV installation up to 8.7 MW in 2050 and starting with 10% of this capacity in 2020. In the model this gave a capacity of 5.5 MW for the final planning period, corresponding to an implemented PV area of 23 521 m^2 and a yearly production of 5.26 GWh. The capacity in

Table 3
The allowed charging and discharging of the STES per season and day, as well as the daily heat demand.

	Charge/discharge per season/day [MWh]	Daily heat demand [MWh]	Share of demand covered by STES
Spring	−500/−9.6	38.2	25%
Summer	13 000/102.4	22.6	–
Autumn	−1400/−22.6	34.7	65%
Winter	−6050/−49.2	53.1	93%
Peak	−50/−50.0	80.0	63%

Table 4
Investment costs and lifetimes for the different alternative technologies, and which technologies need to be invested in each heat supply solution (HTDH - high-temperature DH, LTDH - low-temperature DH).

			Must (can) be included in		
	Costs [M€]	Lifetime [y]	Electric heating	HTDH	LTDH and STES
New transformer	1.0	40	(X)	(X)	(X)
Local heating network	1.9	30		X	X
STES	7.2	60			X
Connection to DH network	3.9	30		X	X
Upgrading existing buildings	97	30	(X)	(X)	(X)

2050 is derived from an analysis done using the GENeSYS-MOD model[2] for different areas in Norway [39] and scaled down based on the expected population at Furuset. In addition to the expected increase in the amount of implemented PV panels over the planning period, the availability of solar energy obviously varies over the year. In the model, separate PV energy sources were thus included for each season and investment period, as shown in Fig. 2.

3.3.4. Building retrofit

Retrofitting has been considered as a measure to reduce the energy demand of the existing housing cooperatives at Furuset, corresponding to a heated area of 115 600 m^2 (approximately 24% of the total building mass). These buildings are and will also in the future be heated with direct electric heating. Upgrading the buildings to passive house standard was estimated to reduce the annual heat demand by 9.8 GWh/year, corresponding to 31% of the non-retrofitted demand, based on calculations with the load profile generator (see section 3.1). In the model it was assumed that retrofitting reduces the heat demand evenly during the heating season (autumn, winter, peak and summer), which corresponds to a reduction of 1.7 MWh/h. Investment costs for renovation were estimated to 900 €/m^2.

3.4. Investment alternatives

The technologies that the model can invest in and their costs are listed in Table 4. The table indicates also which investments the studied three alternative heat supply solutions can or must have. Combinations of four investment alternatives are considered in the context of the increasing load in the area: a larger transformer, connection to the main DH network, a local heating network, a STES, and retrofitting the existing buildings. Local PV production was not considered as an investment option since PV will nevertheless be integrated in some of the buildings at Furuset. Investments in infrastructure inside the buildings, such as electric heaters and hydronic heating are not considered.

The investment costs for the STES and the DH infrastructure were obtained from the DH supplier. The investment in the STES includes costs for the borehole TES and the required heat central. Government support for the STES was not considered in this socio-economic analysis.

The analysis was set up such that the investment in local heating network, STES and connection to the DH network had to be done during the second investment period (in 2030), according to the development plan for Furuset.

4. Results

Table 5 presents the results for annuity from the investment analysis for the scenarios with and without PV (PV and ~~PV~~). Direct electric heating requires no investments, and has thus the lowest total costs, even if the operational costs are highest for this alternative. The alternatives with DH are less than 3% more expensive than the direct electric heating alternative, and these two alternatives have almost the same total costs. Low-temperature DH and STES has clearly the lowest operational costs of all the alternatives.

Table 5
Investment and operational costs from the Integrate runs (M€).

	PV			~~PV~~		
	Operation	Investments	Total	Operation	Investments	Total
Electric heating	2.736	0.000	2.736	2.841	0.0	2.841
HTDH	2.612	0.199	2.812	2.717	0.199	2.917
LTDH and STES	2.414	0.399	2.813	2.516	0.399	2.915

[2] https://openentrance.eu/2021/04/27/genesys-mod-tu-berlin/.

In the ~~PV~~ scenario, the alternative with the STES is slightly less expensive than without.

In any of the 3 investment alternatives, no investment was made in a new transformer or building retrofit. Transformer is unnecessary due to good capacity in the power grid, while upgrading the existing building stock is too expensive to be selected (see Table 4). The results of Table 5 as well as the corresponding results from the sensitivity analyses can also be found on Fig. 7 in the appendix.

4.1. With PV

Table 6 shows the annual delivered energy as well as the peak demand for electricity and DH in the three alternative heat supply options for the PV scenario. When investing in DH (high- or low-temperature), the annual demand for supplied electricity is reduced by 26%, and the peak power requirement is reduced by 28%. When investing in low-temperature DH and STES, the amount of delivered DH increases by 28% annually due to heat losses in the STES, however the peak load requirement is reduced by 31%.

Fig. 5 shows the aggregated breakdown of the energy supplied from different sources for summer and peak periods in the three heat supply alternatives: electric heating, high-temperature DH and low-temperature DH. In the summer, there's a substantial amount of electricity supplied from local PV production. In the low-temperature DH alternative, the amount of import from DH is high in the summer due to charging of the STES.

On the peak day, high heating demand increases the peak power demand in the alternative for direct electric heating. In the high-temperature DH alternative, the peak power demand is reduced due to the heating load (47% of the building mass) that is allocated to the local heating network. In the low-temperature DH alternative, heat from the STES is applied to cover the heating demand

Table 6
Total annual and peak energy demand for electricity and DH in the PV scenario.

	Electricity		DH	
	Energy [GWh/year]	Peak [MWh/h]	Energy [GWh/year]	Peak [MWh/h]
Electric heating	59.2	17.0	0.0	0.0
HTDH	44.0	12.2	16.2	5.22
LTDH and STES	44.0	12.2	20.9	3.61

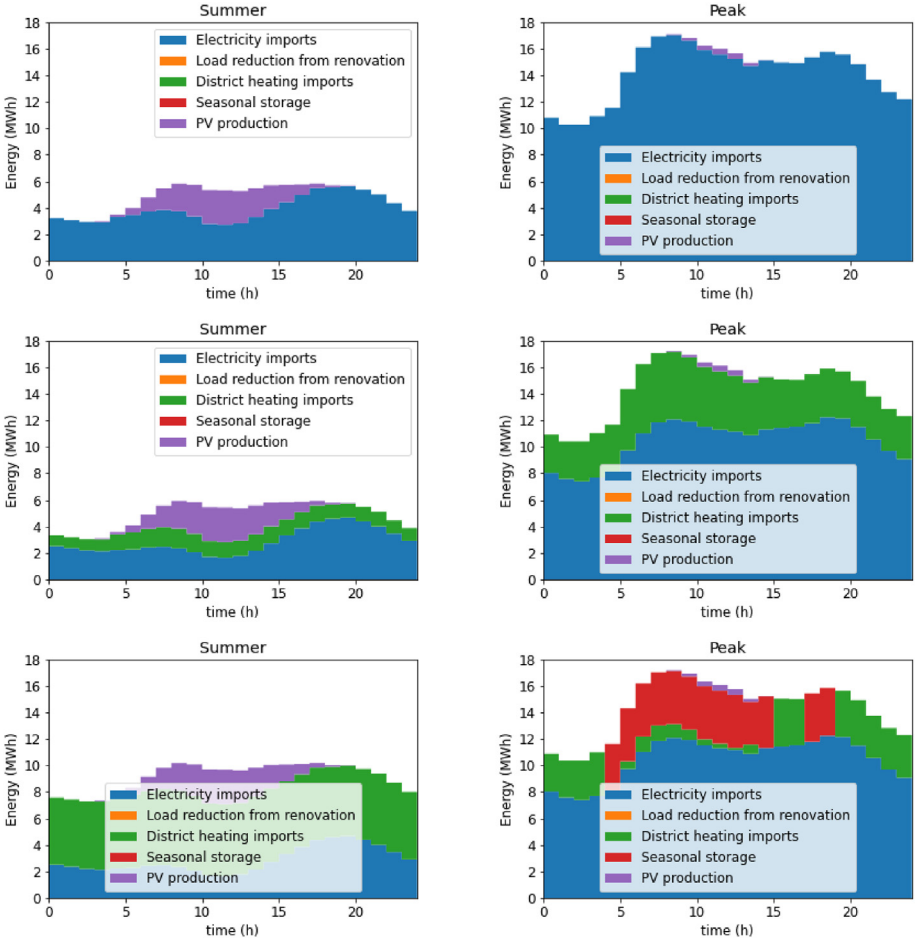

Fig. 5. Energy supply from the different sources in the representative days for summer (left) and peak (right panel), for the investment alternatives of direct electric heating (top row), high-temperature DH (middle row) and low-temperature DH with STES (bottom row) in the PV scenario.

Table 7
Total annual and peak energy demand for electricity and DH in the PV scenario.

	Electricity		DH	
	Energy [GWh/year]	Peak [MWh/h]	Energy [GWh/year]	Peak [MWh/h]
Electric heating	64.3	17.1	0.0	0.0
HTDH	49.1	12.2	16.2	5.22
LTDH and STES	49.2	12.2	20.7	3.91

during the hours when the DH prices are highest, reducing the peak demand from the main DH network.

4.2. Without PV

Table 7 shows the annual delivered energy as well as the peak demand for electricity and DH in the three alternative heat supply options for the ~~PV~~ scenario. The electricity imports are 8.6% and 11.6% higher in the electric heating and DH cases, respectively, due to the absence of PV. The peak electricity imports remain unchanged. The annual imports and peak imports from the DH network are also unchanged.

4.3. Heat losses and pumping power

An important benefit in low-temperature DH is the reduction in heat losses. The annual heat losses were 1.14 GWh (7.5% of the total heat demand) with high-temperature DH, and 0.85 GWh (5.6% of the total heat demand) with low-temperature DH. Energy demand for pumping is twice as high for low-temperature DH (0.031 GWh) as opposed to high-temperature DH (0.014 GWh); however, this energy demand is generally very small (0.20/0.09% of the total heating demand for low-/high-temperature DH).

4.4. Levelized cost of heat

A common metric for comparing different energy production technologies is the levelized cost of energy, or in this case, levelized cost of heat (LCOH). LCOH was calculated for the alternatives with DH according to the formula

$$LCOH = \frac{I_0 + \sum_{t=1}^{n} \frac{C_t}{(1+r)^t}}{\sum_{t=1}^{n} \frac{E_t}{(1+r)^t}} \quad (19)$$

where I_0 is the total initial investment, C_t is the annual operational costs (i.e., the energy costs), E_t is the annual amount of heat delivered by the heat central, n is the number of years of operation, set to 30 years, and r is the interest rate, set to 3%.

The resulting LCOH was 51.9 €/MWh for the high-temperature DH alternative, and 51.5 €/MWh for the STES alternative with low-temperature DH and STES. The average price for DH in Norway in 2020 was 58.1 €/MWh (excluding taxes), and the average power price for Norway in 2020 was 49.3 €/MWh (excluding taxes and charges). 2020 was a year with especially low electricity prices; in 2021, the power prices have doubled, with a price of 79.3 €/MWh for the third quarter.

The obtained values for LCOH are higher than in a previous study on a borehole TES system storing excess heat from waste incineration [19], where LCOH in the range from 10.5 to 23.5 €/MWh was obtained. In this study, the share of heating demand covered by waste heat was in the range of 37.4–89.1% and storage efficiency between 48.1 and 69.2%. The borehole TES volumes considered in this study were 300 000 and 600 000 m^3, and higher storage efficiencies were obtained with smaller storage volumes. In the present study, the storage volume was approximately 5 000 000 m^3, the share of heating demand covered by surplus heat was 54.6%, and storage efficiency 61.5%. The discrepancy in LCOH can thus be partly explained with the lower waste heat utilization factor, and partly by higher investment costs: the cost for boreholes and piping in Ref. [19] were assumed to be 33.5 €/m, while in the present study the costs were 45.9 €/m (including total system costs).

It should be noted that the LCOH calculated here considers heat delivery to the buildings connected to the local heating network, corresponding to ca. 47% of the total heating demand (see section 3). Connecting several buildings to the network would increase the amount of delivered heat, thus reduce the LCOH.

4.5. Sensitivity analyses

4.5.1. STES heat availability

The selected allocation of heat available from the STES in the different seasons shown in Table 3 was based on mere assumptions. In reality, the temperature of the storage might be lower and thus less heat can be extracted e.g. on the peak day. In Ref. [40], the operation of the borehole STES planned at Furuset was evaluated using dynamic simulations. Outcomes of the study include the development of outlet temperatures from the STES to the local heating network over the heating season, as well as the demand for importing heat for different approaches for discharging the STES. To evaluate the sensitivity of the results in the present study to heat availability, an alternative setup with reduced availability during the winter and peak periods was evaluated, based on the outcomes of the study by Jokiel et al. [40]. This setup is shown in Table 8.

The impact of this change on the investment analysis is minimal, with 2.415 M€ for operational costs and 0.40 M€ for investment costs. This results in total costs of 2.81 M€, which is the same as in the previous setup for heat availability in the STES. The reason for the small change in costs is that the storage is still able to cover the demand during the hours when the heat costs are the highest (see

Table 8
The allowed charging and discharging of the STES per season and day with reduced availability in winter and peak periods.

	Charge/discharge per season/day [MWh]	Share of demand covered by STES
Spring	−596/−11.5	63%
Summer	13 000/102.4	–
Autumn	−2108/−34.0	98%
Winter	−5271/−42.9	81%
Peak	−24/−24	30%

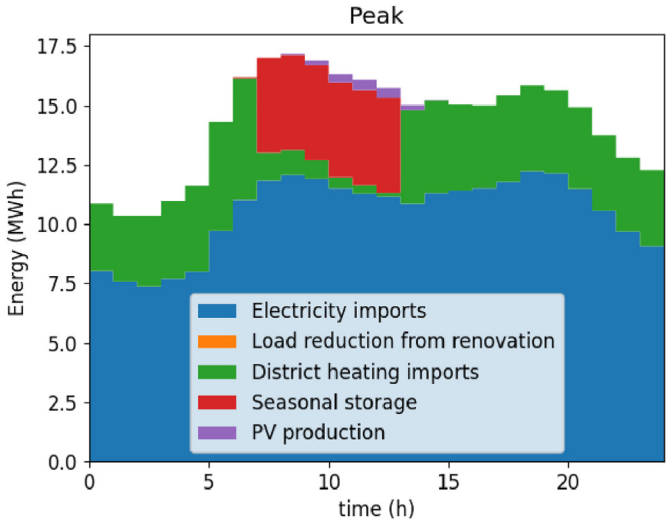

Fig. 6. Energy supply from the different sources on the peak day with low-temperature DH and STES, with reduced availability of heat during winter and peak periods.

Fig. 4(b)), as shown in Fig. 6. The peak demand for DH however increases to 5.11 MWh/h, which is almost the same as without the STES.

4.5.2. STES investment costs

The sensitivity of the results to the investment cost of the STES was studied in order to find out at which point low-temperature DH and STES becomes more cost-effective than to not invest in anything and only use electric heating. The results are presented in Table 9. In both the PV and ~~PV~~ scenarios, low-temperature DH with STES becomes more cost-effective for cost reductions of the STES of slightly less than 40%. Indeed, the total costs in the cases with electric heating were 2.74 and 2.84 M€ for the PV and ~~PV~~ case respectively, corresponding to a required reduction of 38.5 and 37% in the cost of STES.

The storage planned at Furuset is large compared to other existing projects [41] and benefits from an economy of scale. This is not enough to make it competitive to direct electric heating in a non-constrained grid such as Furuset (see the results in Table 5). Reduction in the STES investment costs does, however, have a large impact on the LCOH, with 20% reduction yielding a LCOH of 46.7 €/MWh, and 40% reduction a LCOH of 41.8 €/MWh. Both values are below the average power price in Norway for 2020, which was a year with low power prices.

4.5.3. Reduced grid capacity

We also look at the impact that a reduced grid capacity would have on operational and investment costs. The grid capacity available at Furuset is particularly high (22.6 MW), and represent a special case rather than the normal situation in Oslo. The results from a lowered grid capacity, with a reduction between 3 and 15 MW, are presented in Table 10.

In the direct electric heating case with PV, the operational cost increases with reducing grid capacity due to the deficit penalty, as the capacity becomes too small to cover the peak demand. Low-temperature DH with STES becomes competitive with a grid capacity reduction above 9 MW. Going from 9 to 12 MW reduction in the grid size leads to a 54% increase in operational and total costs for direct electric heating. In the case with low-temperature DH and STES, the investment in the heating network is done earlier, reducing the operational cost, avoiding deficit but increasing slightly the investment cost, leading to an overall 3.6% cost increase. The situation is the same in the ~~PV~~ case, with even larger deficits than in the direct electric heating case. Between 12 and 15 MW grid capacity reduction, the DH and STES is not enough to compensate for the lacking demand.

Investment in a large transformer is not considered here, but the annuity for investing in this alternative is 0.58 M€ and would be more competitive than DH and STES under our cost assumptions.

Table 9
Annuity of investment and operation resulting from a given reduction in the STES investment cost in both the PV and ~~PV~~ scenarios in M€. "Base" represents the cost assumption used in the main analysis.

	PV			~~PV~~		
	Operation	Investments	Total	Operation	Investments	Total
Base	2.414	0.399	2.813	2.516	0.399	2.915
−20%	2.414	0.359	2.773	2.516	0.359	2.875
−40%	2.414	0.319	2.733	2.516	0.319	2.835

4.5.4. Higher winter electricity prices

In 2021, particularly high electricity prices were experienced in many parts of Europe. This can occur for various reasons: increasing level of renewable energy sources combined with unfavorable weather conditions, geopolitical and economical instability affecting gas prices, and high carbon prices to name a few. Those conditions remain rare events, but could become more frequent due to the impact of climate change. In this section, the impact of higher electricity price on the investment alternatives is studied. We consider a price of electricity twice as high as in the rest of the study for the winter and peak seasons, while the prices for the rest of the year are kept unchanged. The corresponding increase in DH costs due to higher costs of using electric boilers and heat pumps is also taken into account. Table 11 presents the resulting investment and operational costs.

As a result of higher electricity prices, low-temperature DH with STES becomes the least cost solution followed by high-temperature DH. The investment in DH alone or in combination with the STES take place in the first period.

4.6. Emission reduction due to implementation of STES

Even if direct electric heating is the option with the lowest socio-economic costs, STES has an important function in reducing the use of peak heating boilers in the main DH network in the winter – thus lowering emissions and costs related to DH production. This effect is not reflected in the modeling results, and thereby a simple calculation on the reduction in emissions was carried out.

In the summer, waste incineration is the only source of heat in the DH network. In the winter, it represents 30% of the heat supply, while the remaining demand is covered with electric boilers, heat pumps, gas and biodiesel (see Table 13 in the Appendix). Investing in the STES allows to use heat that would otherwise not have been utilized and reduces the emissions due to the use of peak heating sources. Table 12 presents the annual emissions[3] for the period 2039–2049 for the different investment alternatives and the contribution of electricity and DH. The emissions from DH in the different seasons are calculated based on the share of each heating technology used.

[3] Based on an emission factor of 277 kg/MWh for gas, 50 kg/MWh for biodiesel, 40 kg/MWh for wood pellets and 17 kg/MWh for electricity [42].

Table 10
Annuity of investment and operational costs resulting from a given reduction in the grid capacity in both the PV and ~~PV~~ scenarios in M€. The second column contains the grid connection reduction from the base value.

		PV			~~PV~~		
		Operation	Investments	Total	Operation	Investments	Total
Electric heating	−3 MW	2.735	0	2.735	2.841	0	2.841
	−6 MW	2.737	0	2.737	2.843	0	2.843
	−9 MW	2.805	0	2.805	2.915	0	2.915
	−12 MW	4.321	0	4.321	5.263	0	5.263
	−15 MW	34.40	0	34.40	38.06	0	38.06
LTDH + STES	−3 MW	2.414	0.399	2.813	2.516	0.399	2.915
	−6 MW	2.414	0.399	2.813	2.516	0.399	2.915
	−9 MW	2.414	0.399	2.813	2.516	0.399	2.915
	−12 MW[a]	2.343	0.571	2.914	2.445	0.571	3.016
	−15 MW[a]	4.661	0.571	5.232	5.858	0.571	6.429

[a] Investment in DH in 2019 and STES in 2029.

Table 11
Investment and operational costs from the Integrate runs with doubled electricity costs in the winter and peak (M€).

	PV			~~PV~~		
	Operation	Investments	Total	Operation	Investments	Total
Electric heating	4.098	0.000	4.098	4.216	0.0	4.216
HTDH	3.609	0.372	3.981	3.728	0.372	4.099
LTDH and STES	3.152	0.755	3.907	3.265	0.755	4.020

Connecting to the DH network allows a reduction of 7−8% of the emissions while the addition of the STES and the increased use of waste heat from the summer leads to a 20% reduction from the base case. The results from Table 12 shows also the contribution of PV in reducing emissions (−8%), which is relatively low due to the low emission factor of electricity in Norway.

5. Discussion and conclusions

Considering the high share of heat produced by waste incineration in the Nordic countries [15−18], there is undoubtedly a high potential for seasonal storage of the excess heat that is produced in the summer due to lack of possibilities for storing waste. In this study, a techno-economic optimization tool was applied to show that utilizing the stored excess heat to cover heating demands of a neighborhood in Norway during the heating season can enable significant reductions in heating costs as well as emissions related to heat production. The investment costs of borehole TES systems for seasonal storage of heat limit the profitability of this solution as compared to more conventional alternatives, such as direct electric heating and high-temperature DH which were used for comparison in this study. However, it was shown that high electricity prices in the winter, and limitations in the grid capacity improve the profitability of STES and DH significantly. This is an important result, considering that both of these scenarios have become very relevant in the recent years with increasing electrification and share of variable renewable sources in the grid.

Table 12
Annual emissions for the energy system considered with the different investment alternatives from electricity and DH (*ton CO_2/year*).

	PV			~~PV~~		
	El.	DH	Total	El.	DH	Total
Electric heating	1007	0	1007	1094	0	1094
HTDH	748	182	930	835	182	1017
LTDH and STES	748	46	794	836	44	880

If STES technology was widespread, it would probably also affect the need for investment in transmission networks. The Norwegian grid operator stands in front of huge investments to meet expected growth in consumption [43], which will be largest in big cities and on the coast. The power grid in Norway is dimensioned based on the highest demand, and since large share of the heating demand is covered with electricity, the grid is heavily loaded during the coldest days of the year. A technology that reduces electricity consumption in general and in particular the peak loads in cities can therefore be very useful. It can thus be concluded that investments in DH and STES can become an important measure to reduce the demand for grid investments and hedge against increasing energy prices and volatility.

The Norwegian energy supply system is quite unique in Europe. The high share of hydro power, combined with a domestic production that exceeds the consumption on an annual basis in a normal year, allows low electricity prices that has lead to more electric heating than in the rest of Europe. It also reduces the scope of the transition necessary for the Norwegian power system to reduce domestic emissions. At the same time, Norway's hydro power resources can play a major role in balancing for variable power production from wind and PV in Europe and consequently reducing the power prices [44]. Reducing the burden on the Norwegian power grid through increased utilization of DH for covering the heating demands would free more of the available hydro power capacity for this purpose, and at the same time reduce or delay grid investments. Widespread implementation of STES would additionally reduce the peak load demands in a DH network, including the use of power-to-heat units (electric boilers and heat pumps) that cover a high share of the heating demand during winter (see Table 13), thus further reducing the load on the power grid and

increasing the system flexibility during periods with high load.

A limitation of the seasonal storage model applied in the present study is that the total storage capacity as well as the allowed charge/discharge of heat per season are user-defined inputs. The storage capacity and yearly charging patterns are hence predefined and cannot be optimized. This poses a challenge as it requires good understanding of the technology from the modeler to ensure sensible input arguments for charge/discharge of heat as well as the heat losses. Moreover, the module does not consider the heat exchange process or the temperature level in the storage, which might lead to an overestimation of heat availability on e.g. the peak day. Still, such high level of detail might be unrealistic in an investment optimization model. A sensitivity analysis carried out on reduced heat availability from the STES on the peak day showed little impact on the economic analysis, although the benefit of reducing peak demand from the DH network was lost. Further work could attempt to address these issues by improving the formulation of long-term storage in the model, and finding a strategy to include the allowed charging/discharging per season as a part of the overall optimization. This would, however, require major modifications to the model or limit greatly the complexity of the modeled energy system. Another approach, and a step further from what is done in this paper, could be to link the model to a more detailed thermal storage model.

Another highly relevant topic for further work could include studying the widespread implementation of STES in e.g. Oslo, and consequently to evaluate its impacts on future grid investments. It would additionally be very interesting to assess the applicability of this technology on European scale in mitigating the seasonal variability in energy prices in a power system with high share of renewable energy sources.

To summarize, the main conclusions from the study are:

1. District heating has a significant impact in alleviating the pressure on the power grid. STES reduces the peak load demands in a DH network, including the use of power-to-heat units, thus further reducing the load on the power grid.
2. STES is not cost optimal under the conditions assumed, however, the total costs were slightly higher compared to electric heating. It was shown that high electricity prices in the winter, and limitations in the grid capacity can render the solution competitive.
3. Investments in DH and STES can become an important measure to reduce the demand for grid investments and hedge against increasing energy prices and volatility.

Declaration of competing interest

The authors declare that they have no known competing financial interests or personal relationships that could have appeared to influence the work reported in this paper.

Acknowledgment

This work has been carried out as a part of the Research Centre on Zero Emission Neighbourhoods in Smart Cities (FME ZEN) funded by the Research Council of Norway (grant agreement No. 257660), as well as the Horizon 2020 project openENTRANCE (grant agreement No. 835896). The authors gratefully acknowledge the support from the Research Council of Norway and the European Union.

Appendix

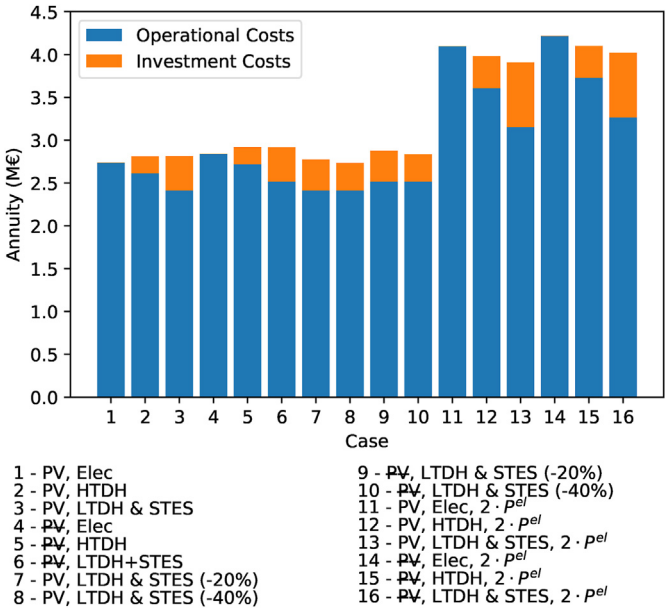

Fig. 7. Graphical summary of the results presented in Tables 5, 9 and 11.

Table 13
The share of heat from the different heat generation units during the different seasons.

	Waste	El.boiler	Heat pump	Pellets	Biodiesel	Gas boiler
Spring	78%	13%	7%	2%	0%	0%
Summer	100%	0%	0%	0%	0%	0%
Autumn	68%	15%	12%	4%	1%	1%
Winter	45%	33%	10%	8%	1%	3%
Peak	30%	30%	10%	18%	6%	6%

References

[1] DNV. Energy transition outlook 2021: a global and regional forecast to 2050. DNV, Tech. Rep.; 2021 [Online]. Available: https://eto.dnv.com/2021.
[2] Mathiesen BV, Lund H, Connolly D, Wenzel H, Østergaard PA, Möller B, Nielsen S, Ridjan I, Karnøe P, Sperling K, et al. Smart energy systems for coherent 100% renewable energy and transport solutions. Appl Energy 2015;145:139–54.
[3] Connolly D, Lund H, Mathiesen BV. Smart energy europe: the technical and economic impact of one potential 100% renewable energy scenario for the European Union. Renew Sustain Energy Rev 2016;60:1634–53.
[4] Lund H, Werner S, Wiltshire R, Svendsen S, Thorsen JE, Hvelplund F, et al. 4th Generation District Heating (4GDH). Integrating smart thermal grids into future sustainable energy systems. Energy 2014;68:1–11. https://doi.org/10.1016/j.energy.2014.02.089.
[5] Heat roadmap Europe, "heating and cooling facts and figures," heat roadmap Europe, tech. Rep [Online]. Available: https://heatroadmap.eu/wp-content/uploads/2019/03/Brochure_Heating-and-Cooling_web.pdf; 2017.
[6] Pezzutto S, Croce S, Zambotti S, Kranzl L, Novelli A, Zambelli P. Assessment of the space heating and domestic hot water market in europe—open data and results. Energies 2019;12(9):1760.
[7] Persson U, Möller B, Werner S. Heat Roadmap Europe: identifying strategic heat synergy regions. Energy Pol 2014;74:663–81.
[8] Wheatcroft E, Wynn H, Lygnerud K, Bonvicini G, Leonte D. The role of low

temperature waste heat recovery in achieving 2050 goals: a policy positioning paper. Energies 2020;13(8):1–19.
[9] Lund H, Østergaard PA, Connolly D, Ridjan I, Mathiesen BV, Hvelplund F, Thellufsen JZ, Sorknæs P. Energy storage and smart energy systems. Int. J. Sustain. Energy. Plann. Manag. 2016;11:3–14.
[10] Yang T, Liu W, Kramer GJ, Sun Q. Seasonal thermal energy storage: a techno-economic literature review. Renew Sustain Energy Rev 2021;139:110732. https://doi.org/10.1016/j.rser.2021.110732.
[11] Gao L, Zhao J, Tang Z. A review on borehole seasonal solar thermal energy storage. Energy Proc 2015;70:209–18.
[12] Mesquita L, McClenahan D, Thornton J, Carriere J, Wong B. Drake landing solar community: 10 years of operation. In: ISES conference proceedings; 2017. p. 1–12.
[13] Hirvonen J, ur Rehman H, Sirén K. Techno-economic optimization and analysis of a high latitude solar district heating system with seasonal storage, considering different community sizes. Sol Energy 2018;162:472–88. https://doi.org/10.1016/j.solener.2018.01.052.
[14] Nordell B, Andersson O, Rydell L, Scorpo AL. Long-term performance of the htbtes in emmaboda, sweden. In: Greenstock 2015: international conference on underground thermal energy storage 19/05/2015-21/05/2015; 2015.
[15] Schweiger G, Rantzer J, Ericsson K, Lauenburg P. The potential of power-to-heat in swedish district heating systems. Energy 2017;137:661–9.
[16] Fruergaard T, Christensen TH, Astrup T. Energy recovery from waste incineration: assessing the importance of district heating networks. Waste Manag 2010;30(7):1264–72.
[17] Energiateollisuus. Energiavuosi 2020 - kaukolämpö. https://energia.fi/files/5650/Kaukolampovuosi_2020_netti_kj_paivitetty_20210318.pdf. [Accessed 28 October 2021].
[18] Fjernvarme Norsk. Fjernvarme - Energikilder 2020. https://www.fjernkontrollen.no/. [Accessed 28 October 2021].
[19] Hirvonen J, Kosonen R. Waste incineration heat and seasonal thermal energy storage for promoting economically optimal net-zero energy districts in finland. Buildings 2020;10(11):1–19.
[20] Connolly D, Lund H, Mathiesen BV, Leahy M. A review of computer tools for analysing the integration of renewable energy into various energy systems. Appl Energy 2010;87(4):1059–82.
[21] Steen D, Stadler M, Cardoso G, Groissböck M, DeForest N, Marnay C. Modeling of thermal storage systems in MILP distributed energy resource models. Appl Energy Jan. 2015;137:782–92.
[22] Schütz T, Streblow R, Müller D. A comparison of thermal energy storage models for building energy system optimization. Energy Build Apr. 2015;93:23–31.
[23] Bachmaier A, Narmsara S, Eggers J-B, Herkel S. Spatial distribution of thermal energy storage systems in urban areas connected to district heating for grid balancing—a techno-economical optimization based on a case study. J Energy Storage 2016;8:349–57.
[24] Romanchenko D, Nyholm E, Odenberger M, Johnsson F. Balancing investments in building energy conservation measures with investments in district heating – a Swedish case study. Energy Build Nov. 2020;226:110353.
[25] Buoro D, Pinamonti P, Reini M. Optimization of a distributed cogeneration system with solar district heating. Appl Energy Jul. 2014;124:298–308.
[26] Gabrielli P, Gazzani M, Martelli E, Mazzotti M. Optimal design of multi-energy systems with seasonal storage. Appl Energy 2018;219:408–24. https://doi.org/10.1016/j.apenergy.2017.07.142 [Online]. Available:.
[27] WEDISTRICT. Interactive map: share of district heating and cooling across europe. https://www.wedistrict.eu/interactive-map-share-of-district-heating-and-cooling-across-europe/. [Accessed 11 February 2022].
[28] Bakken BH, Skjelbred HI, Wolfgang O. etransport: investment planning in energy supply systems with multiple energy carriers. Energy 2007;32(9):1676–89 [Online]. Available: https://www.sciencedirect.com/science/article/pii/S0360544207000175.
[29] Kvalsvik K, Kauko H. "Linear optimization of district heating systems: description of an upgraded district heating module for eTransport," ZEN Report No. 9 [Online]. Available: https://fmezen.no/wp-content/uploads/2018/12/ZEN-Report-no-9_optimisation-district-heating.pdf; 2018.
[30] Kauko H. "Integrate district heating module: user guide and technical documentation," ZEN Memo No. 34 [Online]. Available: https://fmezen.no/wp-content/uploads/2021/10/ZEN-Memo-34-DH-module-v4.pdf; 2021.
[31] Kauko H. eTransport modules for diurnal and seasonal heat storage. ZEN Memo; 2019.
[32] Daniela B, Andresen I. ZEN pilot projects: mapping of the pilot projects within the Research Centre on Zero Emission Neighbourhoods in Smart Cities. ZEN Report 2018;10.
[33] Fortum Oslo Varme. Storskala demonstrasjon av fremtidens energisystem: Furuset mikroenergisystem. Project description; 2019.
[34] Kauko H, Wolfgang O, Pinel D. "Sesonglagring av varme for lokale energisystem – analyse av potensialet på Furuset," ZEN Report No. 35 [Online]. Available: https://fmezen.no/wp-content/uploads/2021/11/ZEN-Report-35_SESONGLAGRING-AV-VARME-FOR-LOKALE-ENERGISYSTEM-1.pdf; 2021.
[35] Lindberg KB, Bakker SJ, Sartori I. Modelling electric and heat load profiles of non-residential buildings for use in long-term aggregate load forecasts. Util Pol 2019;58:63–88.
[36] Lund K, Skrivarhaug AV. "Langsiktig kraftmarkedsanalyse 2020 – 2040," the Norwegian water resources and energy directorate (NVE), tech. Rep [Online]. Available: http://publikasjoner.nve.no/rapport/2020/rapport2020_37.pdf; 2020.
[37] Lovinda Ødegården SB. "Status og prognoser for kraftsystemet 2018," the Norwegian water resources and energy directorate (NVE), tech. Rep [Online]. Available: https://publikasjoner.nve.no/rapport/2018/rapport2018_103.pdf; 2018.
[38] DNV GL Energy. Strømnettet i et fullelektrisk Norge. 2019. Energi Norge, Tech. Rep. 2019-0218. [Online]. Available: https://www.energinorge.no/contentassets/74f33e5598d64578bda89c1fa864e83a/rapport-stromnettet-i-et-fullelektrisk-norge.pdf.
[39] Sørbye AH, Weisz SUD. Modeling multi-sectoral decarbonization scenarios for the Norwegian energy system. Master's thesis. NTNU, Department of Electric Power Engineering; 2021.
[40] Jokiel M, Rohde D, Kauko H, Walnum HT. Integration of a high-temperature borehole thermal energy storage in a local heating grid for a neighborhood. In: BuildSIM-Nordic 2020. plus 0.5em minus 0.4emSINTEF. Academic Press; October 2020.
[41] Kallesøe AJ, Vangkilde-Pedersen T, editors. Underground Thermal Energy Storage (UTES) – state-of-the-art, example cases and lessons learned. HEATSTORE project report. GEOTHERMICA – ERA NET Cofund Geothermal; 2019. 130 pp + appendices.
[42] Pinel D, Korpås M, Lindberg KB. Impact of the CO_2 factor of electricity and the external CO_2 compensation price on zero emission neighborhoods' energy system design. Building and Environment 2021;187:107418.
[43] Statnett, "Nettutviklingsplan 2021," https://www.statnett.no/globalassets/for-aktorer-i-kraftsystemet/planer-og-analyser/nup-2021/nettutviklingsplan-2021.pdf.
[44] Graabak I, Jaehnert S, Korpås M, Mo B. Norway as a battery for the future european power system—impacts on the hydropower system. Energies 2017;10(12):2054.